http://dx.doi.org/10.5012/bkcs.2012.33.11.3601

Solvation of a Small Metal-Binding Peptide in Room-Temperature Ionic Liquids

Youngseon Shim,[†,‡,*] Hyung J. Kim,[‡] and YounJoon Jung[†,*]

[†]*Department of Chemistry, Seoul National University, Seoul 151-747, Korea*
[*]*E-mail: ddalgi1231@gmail.com (Y. Shim); yjjung@snu.ac.kr (Y. Jung)*
[‡]*Department of Chemistry, Carnegie Mellon University, Pittsburgh, PA 15213, U.S.A*
Received June 25, 2012, Accepted August 7, 2012

Structural properties of a small hexapeptide molecule modeled after metal-binding siderochrome immersed in a room-temperature ionic liquid (RTIL) are studied *via* molecular dynamics simulations. We consider two different RTILs, each of which is made up of the same cationic species, 1-butyl-3-methylimidazolium (BMI^+), but different anions, hexafluorophosphate (PF_6^-) and chloride (Cl^-). We investigate how anionic properties such as hydrophobicity/hydrophilicity or hydrogen bonding capability affect the stabilization of the peptide in RTILs. To examine the effect of peptide-RTIL electrostatic interactions on solvation, we also consider a hypothetical solvent BMI^0Cl^0, a non-ionic counter-part of BMI^+Cl^-. For reference, we investigate solvation structures in common polar solvents, water and dimethylsulfoxide (DMSO). Comparison of BMI^+Cl^- and BMI^0Cl^0 shows that electrostatic interactions of the peptide and RTIL play a significant role in the conformational fluctuation of the peptide. For example, strong electrostatic interactions between the two favor an extended conformation of the peptide by reducing its structural fluctuations. The hydrophobicity/hydrophilicity of RTIL anions also exerts a notable influence; specifically, structural fluctuations of the peptide become reduced in more hydrophilic BMI^+Cl^-, compared with those in more hydrophobic $BMI^+PF_6^-$. This is ascribed to the good hydrogen-bond accepting power of chloride anions, which enables them to bind strongly to hydroxyl groups of the peptide and to stabilize its structure. Transport properties of the peptide are examined briefly. Translations of the peptide significantly slow down in highly viscous RTILs.

Key Words : Room-temperature ionic liquid, Peptide, Hydrogen bonding, Solvation structure, Molecular dynamics simulation

Introduction

Due to interesting and unique properties of room-temperature ionic liquids (RTILs), they have received considerable interest of research in diverse areas, ranging from chemistry, physics, chemical engineering, and nanoscience and technology. Potential applications of RTILs are not only limited to their original promises in novel solvents but include electrolytes in energy devices and scaffold media for self-assembly processes.

Another area that has gained considerable interest is biotechnological applications of RTILs. Recent studies have shown that RTILs can be profitably used in diverse areas of bio-technology.[1] For example, Fujita *et al.*[2] have reported that a metalloprotein, cytochrome *c*, exhibits enhanced solubility and stability when it is dissolved in dihydrogen phosphate-based ionic liquids. Another examples include the use of RTILs as solvent materials for enzyme reactions. For instance, Candida antarctica lipase B shows much enhanced performances as enzyme, exhibiting higher selectivity, faster reaction rate, and greater stability, when it is dissolved in RTILs than in conventional solvents. This makes it promising to use RTILs in many applications for bio-catalysis.[3] Baker and coworkers[4] showed high thermodynamic stabilization of a sweet protein, monellin in RTIL. Using fluorescence spectroscopy, they found that the unfolding temperature increases substantially when the protein is dissolved in the ionic liquid, 1-butyl-1-methylpyrrolidinium bis(trifluoromethanesulfonyl)imide. In terms of enhanced solubility, starch and zein proteins are found to be soluble at elevated temperatures in ionic liquids such as 1-butyl-3-methylimidazolium chloride and 1-butyl-3-methylimidazolium dicyanamide.[5]

In these examples, RTILs can play active roles in controlling folding behavior of proteins and their aggregates. For example, a recent study shows that the ionic liquid ethylammonium nitrate can prevent aggregation of denatured protein, hen egg white lysozyme, and can enhance the recovery of active protein during the refolding process.[6] An ionic liquid based on imidazolium and chloride can also act as refolding enhancers of the hen egg white lysozyme and the antibody fragment ScFvOx, where hydrophobic imidazolium with longer alkyl chains destabilize the protein.[7]

In terms of molecular viewpoint, unique and enhanced solvating power of RTIL arises from two distinct and competing interactions present: directional, short-ranged hydrogen bonding and undirectional, long-ranged electrostatic interactions. It is these interactions that make solvation structures in RTILs subtle and complex. Computational efforts have been exerted recently toward understanding molecular mechanism of the interactions between biomolecules and RTILs. For example, solvation structure and stability of the

zinc finger protein[8] and ubiquitin protein[9] in hydrated 1-ethyl-3-methylimidazolium trifluoromethanesulfonate ionic liquid have been recently studied by Haberler *et al*. *via* MD simulations. Tome and coworkers performed a MD simulation study for aqueous solutions of five different amino acids in the presence of 1-butyl-3-methylimidazolium bis(trifluoromethyl)sulfonylimide ionic liquid.[10] They exhibited that solvation structure of the amino acid is determined by a balance between the competitive interactions with ions and water according to the hydrophobicity of the amino acid.

Another interesting studies include MD simulation studies on solvation mechanism of DNA in RTILs.[11,12] Cardoso and coworkers showed that the DNA structure is highly stabilized in various RTILs,[11] in agreement with an experimental study.[13] They pointed out that high stability in the solvation structure arises from the hydrogen-bonding interactions of the cations and anions with the DNA bases as well as interactions between the cations and P-O bonds of phosphates in the DNA strands. On the other hand, strong interactions of the solvent ions with enzymes make them less stable and reduce their activity. In several publications, enzymes such as Candida antartica lipase B, Candida rugosa and penicillin G acylase are generally found to show the highest stability in hydrophobic BMI^+ PF_6^- rather than in hydrophilic RTILs such as those with hydrophilic tetrafluoroborate (BF_4^-) and nitrate (NO_3^-) anions.[14-19] For example, Klähn and coworkers demonstrated solvation and stability of a Candida antartica lipase B enzyme in various RTILs *via* MD simulations.[14,20] They found that more hydrophilic and small anions increases their interactions with the lipase, which has a tendency to destabilize the enzyme. An MD simulation study by the Soares group also reported that an enzyme, serine protease cutinase is less stabilized in BMI^+ NO_3^- relative to BMI^+ PF_6^- due to the strong affinity of the nitrate anion toward the protein main chain.[19] Especially, the enzyme is preferentially stabilized in $BMI^+PF_6^-$ with a structure similar to the native one at a specific water content at ambient temperature, and increases their thermostability significantly at high temperature.

Key aspects to understanding of the protein stabilization in RTILs would be the nature of Coulombic interaction, hydrophobic interaction of the nonpolar group, and hydrogen bonding ability. If the anions can form stable hydrogen bonds with the protein backbone strongly, intra-molecular hydrogen bonds that maintain the structural integrity of the helix can be easily disrupted, which results in the unfolding of the protein. On the other hand, strong Coulombic interactions between the peptide and RTIL can be utilized to renature the aggregated protein and recover their protein activity.

In this work we focus on the microscopic origins of solvation structure of small proteins in RTILs by performing MD simulation studies. As a model protein we consider a small metal-binding peptide molecule, commonly found in siderochromes, compounds typically found in bacteria and fungi and are involved in the iron transport process of microbial organisms.[21] The key and common structural motif in siderochromes are ferrichromes. Ferrichrome is a small peptide molecule, composed of six residues arranged in a cyclic hexapeptide structure, and it acts as a strong ferric chelator. Due to its important role in the iron transport process in fungi or bacteria, many experimental studies have been performed in their solvation structure. However, detailed microscopic studies have not been performed toward the understanding of the solvation structure between properties of different types of RTILs.

We address two questions regarding these issues in this work. The first question is how solvation structures of the peptide are affected by different types of solvents. We choose 1-butyl-3-methylimidazolium, water, and dimenthylsulfoxide (DMSO) as a representative RTIL, protic, and aprotic solvent, respectively. Second, we investigate the anionic effect on the conformational fluctuations of peptides by invoking two different types of RTIL with the same BMI^+ cation, but different anions, one with Cl^- and the other with PF_6^-. Finally, to examine the effect of solvent polarity, we also study on the peptide immersed in a hypothetical solvent, BMI^0Cl^0.

The outline of this paper is as follows: We first give a brief description of the model system and simulation methods employed in this study. MD results are compiled in Figure 1-6 and Table 1. Structural properties of the peptide in BMI^+ PF_6^- and BMI^+ Cl^- are analyzed compared with ones in water and DMSO at different thermodynamic conditions. Finally, concluding remarks are given.

Models and Methods

The simulation cell comprises a single hexa-peptide molecule immersed in either 128 pairs of BMI^+ PF_6^- or BMI^+ Cl^- for the RTIL solvation case. The potential parameters are taken from Ref. 22 for BMI^+, and from Refs. 23 and 24 for Cl^- and PF_6^-. Our model peptide is composed of six residues, LYS1-LYS2-LYS3-GLY-SER1-SER2, with a total of 44 heavy atoms. Here, lysine is considered to be mutant of actual δ-*N*-acyl-δ-*N*-hydroxyl-L-ornithine residue in the metal-binding ferrichrysin. N-terminal SER2 is positively charged, while LYS1 is negatively charged as the C-terminal residue. This hexapeptide model (HPM) corresponds to a denatured open structure of mutated cyclic ferrichrysin, obtained by breaking the bond between LYS1 and SER2 in the cyclic structure. The force field parameters for HPM are generated by DL_PROTEIN[25] program using GROMOS-87 37C4 force field.[26] Simulations were conducted in the canonical ensemble at 400K by using DL_POLY program[27] and VMD[28] was used for visualization purpose. The density of the system was obtained from NPT ensemble simulations at 400 K and 1 atm. For reference, the melting points of pure BMI^+ PF_6^- and BMI^+ Cl^- are 283 and 338 K, respectively, and both of them are thermally stable at 400 K.[29] According to several prior MD studies, analysis of RTILs at this temperature seems to provide a reasonable framework to understand their behaviors at lower temperatures but above the melting point.[30] The long-range electrostatic interactions were computed *via* the Ewald method, resulting in essentially no

truncation of these interactions. The trajectories are integrated *via* the Verlet leapfrog algorithm using a time step of 1 fs. We computed averages from configurations collected from five different 2 ns trajectories. Prior to the 2 ns production run, each trajectory was equilibrated for 10 ns after annealing from 800 K. For comparison, systems composed of 512 DMSO molecules and of 512 SPC/E water[31] molecules were simulated at 298 K and 350 K. As for DMSO, P2 model[32] and a flexible model[33] were employed for the inter- and intra-molecular interactions, respectively.

Results and Discussions

Effects of Solvent Polarity. We first examine the structure of our model hexapeptide molecule, HPM, in the gas phase. In a snapshot shown in Figure 1, the employed force field for the model peptide yields a nearly cyclic structure analogous to the native structure for ferrichrome-type siderphores,[21] of which the amino terminal of SER2 and carboxyl terminal of LYS1 are linked together. End-to-end distance between the N-terminal and C-terminal, l_e, is 3.2 Å. Oxygen in the latter binds to hydrogen of the former with an average separation of 2.4 Å between the two. The mass-weighted radius of gyration R_g is defined by

$$R_g^2 = \left\langle \frac{\Sigma_i^N m_i(\vec{r}_i - \vec{r}_{CM})^2}{\Sigma_i^N m_i} \right\rangle, \quad (1)$$

where m_i and $\vec{r}_i$ are the mass and the position vector of the i-th atom in the peptide with N atomic sites, and $\vec{r}_{CM}$ is the center-of-mass of the peptide. <···> denotes an ensemble average. Our model peptide with a cyclic structure gives a small radius of gyration of R_g = 4.1 Å in the gas phase.

Upon solvation in polar solvents, structure of the HPM becomes significantly distorted compared to the gas phase. The influence of the solvent polarity on the peptide structure is investigated by comparing its structures in the gas phase and in solutions. To construct an average structure, we align the coordinates of each recorded peptide configuration with those of the first recorded configuration. This procedure involves translational alignment of peptide configurations so that their centers of mass coincide with each other, followed by a rotational alignment that involves minimization of the root-mean-square deviation (RMSD) of the heavy atoms.[34]

The RMSD (α, β) measures the spatial deviation between atoms of the same type for two different structures denoted by α and β, and is given by

$$\text{RMSD}(\alpha, \beta) = \left[\frac{1}{N} \Sigma_i^N (\vec{r}_{i,\alpha} - \vec{r}_{i,\beta})^2 \right]^{\frac{1}{2}} \quad (2)$$

In calculating RMSD, we first obtain an averaged HPM structure in a solvent by taking an ensemble average of the aligned conformations along the trajectories. Structural distortion of the peptide in solvent can be quantified by calculating RMSD between the averaged peptide structure in the solvent and its gas phase structure. RMSD can also be used to compare structural differences between averaged peptide structures obtained from different solvents.

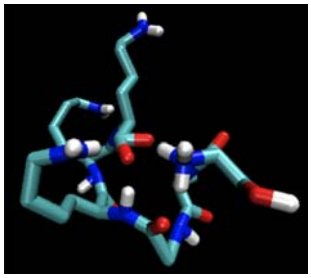

Figure 1. A snapshot of a model ferrichrome in the gas phase.

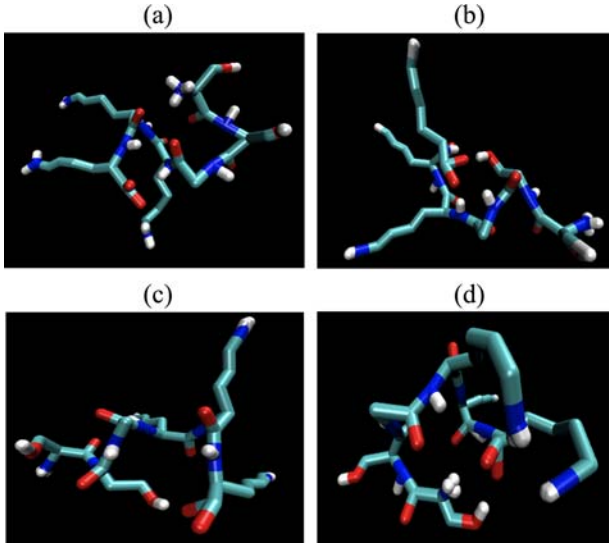

Figure 2. Snapshots of the average peptide structures in (a) BMI^+Cl, (b) $BMI^+PF_6^-$, (c) SPC/E water, (d) BMI^0Cl^0, obtained at 400 K and 298 K for RTILs and water, respectively.

Average peptide structures in different solvents are exhibited in Figure 2. The HPM conformations in BMI^+Cl^- and $BMI^+PF_6^-$ shown in Figure 2(a) are distorted from the isolated structure by RMSD = 1.3 and 2.1 Å, respectively. Solvation in water and DMSO also yields considerable structural changes for the peptide with RMSD = 1.7 Å in both solvents. We also monitor the time-dependent fluctuations of the radius of gyration of our model peptide, $R(t)$, in BMI^+Cl^- and $BMI^+PF_6^-$ in Figure 3(a), and compare with those in SPC/E water in Figure 3(b). Details of the peptide structural change and its fluctuations are compiled in Table 1. The most salient feature is that among all solvents considered here, the HPM forms the most compact structure in BMI^+Cl^- as confirmed by its small mean R_g value (R_g = 4.6 Å) in this RTIL. The fluctuation of R_g, determined as its standard deviation σ, is also the smallest in BMI^+Cl^-. We note that fluctuations of R_g become enhanced at a higher temperature as shown in Figure 3(b) for water, where the trajectory at 350 K is shifted upward by 0.7 Å for clarity. Nonetheless, the σ value at 400 K in BMI^+Cl^- is lower than that at 298 K in water. This result clearly reveals structural stabilization of the peptide in BMI^+Cl^-. We will come back to this point

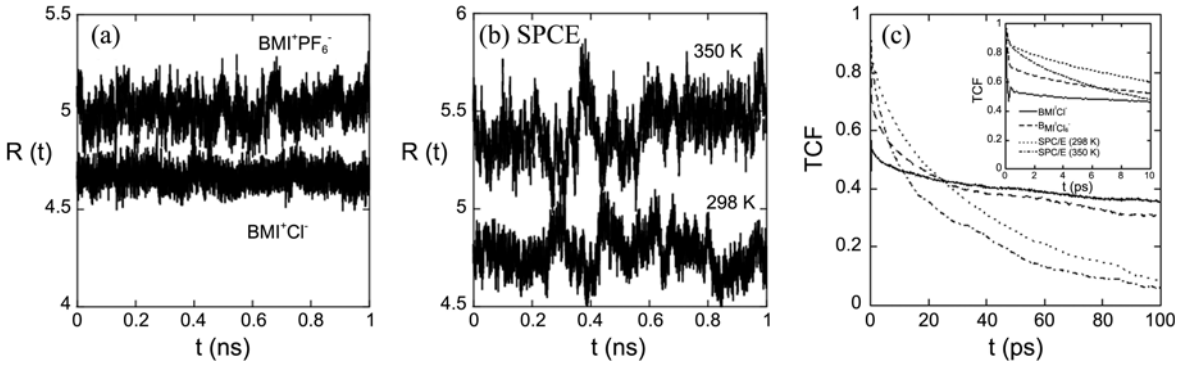

Figure 3. Radius of gyration $R(t)$ of the peptide in (a) RTILs at 400 K and (b) SPC/E water. In (b), $R(t)$ for SPC/E water at 350 K is shifted up by 0.7 Å. (c) Time correlation functions of $R(t)$ obtained in (a) and (b).

below.

Time correlation functions (TCFs) of R_g are considered in Figure 3(c) to examine conformation relaxation of HPM. The conformational correlation time, determined as the area under the normalized TCF, is 220 ps in BMI^+Cl^- and 145 ps in $BMI^+PF_6^-$, while it is 44 and 27 ps in water at 298 and 350 K, respectively. Relaxation of the HPM conformation is much slower in ionic liquids than in water due to high viscosity of the former.

Structural stabilization of the peptide can be further explored at the level of individual residue by calculating root-mean-square fluctuation (RMSF) of the n-th residue defined by

$$\mathrm{RMSF}_n = \left[\frac{1}{M}\sum_{\alpha=1}^{M}(\vec{r}_n(t_\alpha)-\langle\vec{r}_n\rangle)^2\right]^{\frac{1}{2}}, \quad (3)$$

where M is the total number of sampled HPM structures, and $\vec{r}_n$ is the position of the n-th heavy atom of the peptide (n = 1, 2, … 44) and $\langle\vec{r}_n\rangle$ means an ensemble average of their alignments. Results for RMSF are displayed in Figure 4. RMSF values are smaller in RTILs than in water even though the former are at higher temperature than the latter. This reveals high structural stability of the peptide induced by solvation in RTILs, compared to other solvents. We note that BMI^+Cl^- yields the largest structural stabilization of HPM among all solvents considered here. Another notable feature is that RMSF's corresponding to alkyl side-chains (n = 6-9, 15-18, 24-27) of LYS 1-3 are higher than the side

Table 1. Various structural quantities obtained from MD simulation of the peptide in solvents[a]

Solvent (T)	R_g	σ	RMSD	l_e
BMI^+Cl^-(400 K)	4.6	0.056	1.3	5.8
BMI^0Cl^0(400 K)	4.3	0.095	2.0	3.0
$BMI^+PF_6^-$(400 K)	5.0	0.086	2.1	5.3
DMSO(298 K)	5.0	0.10	1.7	6.7
SPC/E(298 K)	4.7	0.12	1.7	6.4
SPC/E(350 K)	4.7	0.14	1.7	6.4

[a]Temperature (T) and length units are K and Å. R_g and l_e of the peptide in the gas phase are obtained to be 4.1 and 3.2 Å.

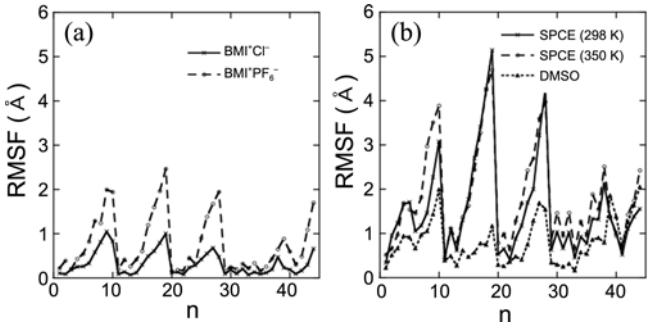

Figure 4. Root-mean-square fluctuations (RMSFs) of the peptide in (a) RTILs at 400 K and (b) SPC/E water.

changes of other residues in all solvents. The non-polar alkyl side-chains frequently change their orientations and explore many different orientations along the trajectory. Such a free orientation of the nonpolar side-chain of the peptide in polar solvent environments was also studied by Garíca and co-workers.[35]

To examine the effect of the electrostatic forces exerted by the RTIL environment, we make a comparison with results obtained in a non-ionic binary system BMI^0Cl^0. This hypothetical solvent is identical to BMI^+Cl^- except that its constituent atoms are all electrically neutral, *i.e.*, they do not interact *via* electrostatic interactions. In Figure 2(d), the peptide in non-ionic BMI^0Cl^0 forms a self-closed structure, distinguished with those in polar solvents. Due to its self-closed structure, the peptide has a small radius of gyration of R_g = 4.3 Å with a standard deviation of 0.095. End-to-end distance, l_e, is 3.0 Å in BMI^0Cl^0, *i.e.*, the carbon atom of the C-terminal and the nitrogen atom of the N-terminal are quite close to each other, while their separation is much larger in other solvents (for details, see Table 1). The structure deviation of HPM in BMI^0Cl^0 compared to BMI^+Cl^- was found to be significant; its RMSD value between the two solvents was calculate to be 2.2 Å. Thus electrostatic interactions with a surrounding solvent provide a more favorable environment for HPM to adopt extended structures and reduce its structural fluctuations. We note, however, that the peptide takes quite a distinct structure in BMI^0Cl^0 from that in the gas phase, as evidenced by RMSD = 2.0 Å from the latter,

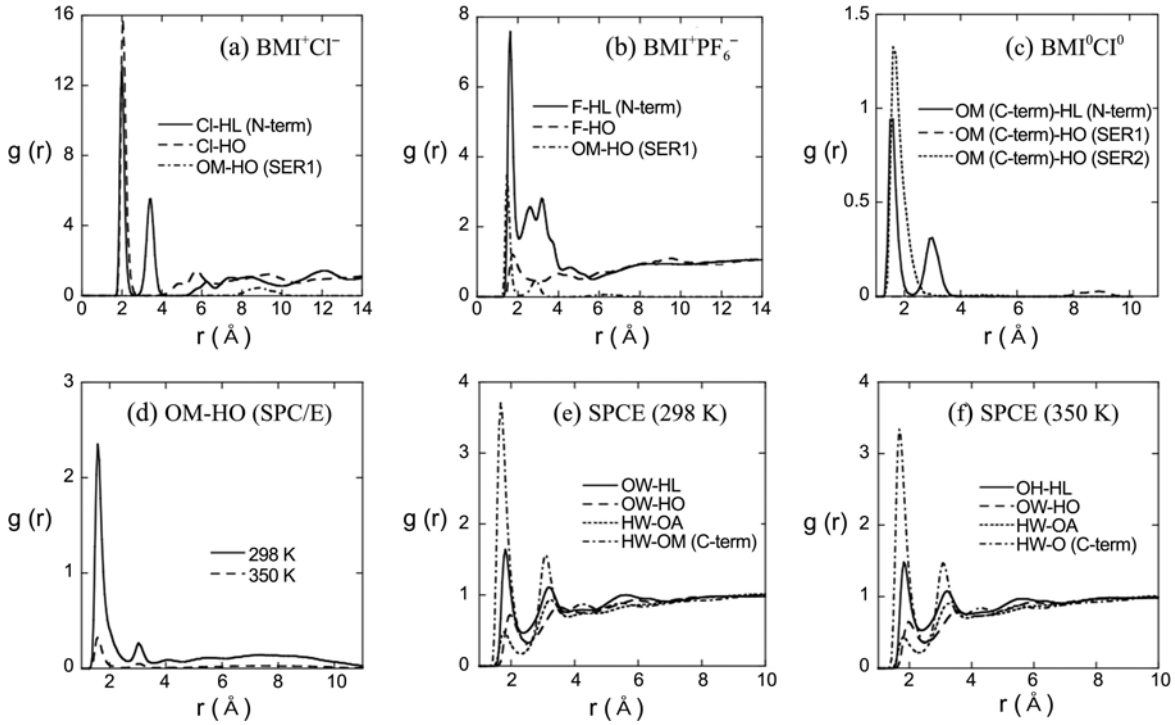

Figure 5. Radial distribution functions $g(r)$ in different solvents; (a) BMI^+Cl; (b) BMI^+PF_6; (c) BMI^0Cl^0; (d)-(f) SPC/E water. OM, HO and HL denote the atomic sites of the peptide, *i.e.*, oxygen, hydrogen, hydrogen of the N-term, respectively. OW and HW are the oxygen and hydrogen sites of SPC/E water. In (d), $g(r)$ is obtained between OM in C-term and HO in SER1 in the peptide.

although they are both close-closed form.

Hydrogen Bonding in Peptide Solvation. To gain additional insight into solvation structure of HPM in different solvents, we consider the radial distribution functions, $g(r)$, in Figure 5. In $BMI^+PF_6^-$, oxygen atoms of C-terminal LYS1 of HPM forms a strong hydrogen-bond with hydroxyl hydrogen of its SER1, as revealed by a peak structure at 1.5 Å plotted in dashed-dot lines in Figure 5(b). The formation of intramolecular, more specifically "intra-protein", hydrogen bonds strongly perturbs the peptide structure compared to the gas phase. As we change RTIL anionic species from PF_6^- to Cl^- (Figure 5(a)), HPM undergoes major structural changes due to hydrophilic nature of the chloride anion. To be specific, BMI^+Cl^- does not allow formation of short-distance intramolecular structure between SER and LYS residues. Instead, Cl^- strongly binds to the hydroxyl hydrogen atom of SER1. The number of chloride ions around the hydroxyl group of SER1, obtained by integrating $g(r)$ in Figure 5(a) up to 3 Å of the first solvation shell, is about one. Cl^- ions also form hydrogen bonds with other hydrogen sites of HPM, for example, hydrogen of the OH-side chain in SER2 or N-terminal. As a result, the peptide structure in BMI^+Cl^- (RMSD = 1.3 Å) is closer to its isolated structure than that in $BMI^+PF_6^-$ (RMSD = 2.1 Å) is. As discussed above, isolated HPM in Figure 1 does not show any intramolecular hydrogen bonds other than the end-to-end hydrogen bond. We suggest that the strong interaction of the hydrophilic Cl^- anion with the hydrogen-bond donors of the peptide, especially the alcoholic group in SER amino acid, is one of the main mechanisms of peptide structural stabilization induced by BMI^+Cl^-. Furthermore, as shown in Figure 3(a) and Figure 4(a), BMI^+Cl^- does not yield significant structural fluctuations in R_g and RMSF for the peptide solvation. Consequently, hydrogen-bond accepting, polar RTILs such as BMI^+Cl^- provide a high structural stability for metal-binding peptides through specific and nonspecific solvation.

In BMI^0Cl^0, both N-terminal and SER2 form hydrogen bonds with the C-terminal LYS1, which are not found in the isolated peptide. This is responsible for large structural deviation of HPM in BMI^0Cl^0 despite its self-closed conformation. As shown in Figure 5(d), a robust hydrogen bond structure between the hydroxyl group of SER1 and oxygen of the C-terminal LYS1 is obtained at a separation of 1.6 Å in water, analogous to $BMI^+PF_6^-$. The strength of this intramolecular hydrogen bond becomes weaker with increasing temperature; the height of the hydrogen bond peak in $g(r)$ decreases by a factor of 7 as the water temperature rises from

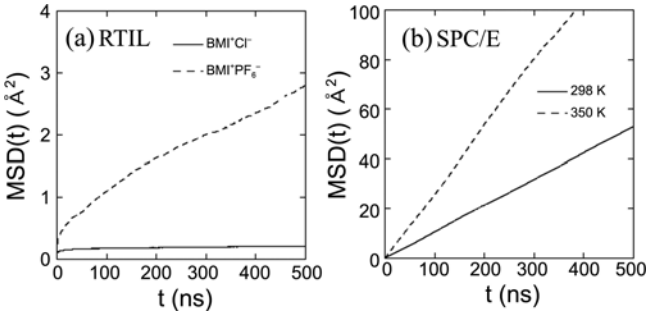

Figure 6. Mean-square displacements (MSD) of the center of the mass of the peptide in (a) RTILs and (b) SPC/E water.

298 to 350 K. Results in Figure 5(e) and (f) show that water molecules also form hydrogen bonds with HPM, in particular, oxygen of C-terminal and hydrogen of N-terminal, which exhibit stronger intermolecular hydrogen bonds than any other sites of the peptide.

In addition to structural studies, transport behavior of the peptide in highly viscous RTIL was examined. Briefly, the mean-square displacement of the peptide in Figure 6 shows that as expected, its translational motions are significantly decelerated in $BMI^+ Cl^-$ and $BMI^+ PF_6^-$, compared to those in water. In $BMI^+ Cl^-$, the center of mass of the peptide is found to be almost trapped, which further confirms the structural stability of the peptide in $BMI^+ Cl^-$.

Concluding Remarks

MD studies on solvation structure of a small metal-binding peptide molecule immersed in room-temperature ionic liquids (RTILs) were presented. Cyclic hexa-peptide structure in the gas phase is significantly distorted in polar solvents and ionic liquids. This solvation-induced conformation change is attributed to electrostatic interactions between the peptide and its surrounding environment. $BMI^+ Cl^-$ provides the most stable environment, resulting in extremely small structural fluctuations of the peptide, even at a high temperature. This is because chloride anions in hydrophilic $BMI^+ Cl^-$ strongly bind to hydroxyl groups of the peptide by dominating over intra-molecular hydrogen bonds found in other solvents. Our study shows that the electrostatic interactions and hydrogen bonding capability of RTILs have a significant influence on the stability of the peptide structure. In relating to other experimental studies, enzymes and proteins in RTILs often maintain their activity and structure over a longer period and at a much higher temperature than in molecular organic solvents. Therefore it is worthwhile to examine free-energetics and related thermal stability of a model peptide in RTILs and compare with other solvents, changing the thermodynamic condition in the near future.

Acknowledgments. We thank Professor Miguel Llinas for suggesting mutated ferrichrysin for this study. This work was supported in part by the National Research Foundation of Korea (NRF) grants funded by the Korea government (MEST) (Nos. 2011-0003555, 2012-0005058, 2012-0000775, and 2011-0013299) and by the KISTI Supercomputing Center (KCS-2011-C1-15 and KSC-2012-C2-47).

References

1. (a) Rantwijk, F. van; Sheldon, R. A. *Chem. Rev.* **2007**, *107*, 2757. (b) Pârvulescu, V. I.; Hardacre, C. *Chem. Rev.* **2007**, *107*, 2615. (c) Yang, Z.; Pan, W. *Enzyme and Microbial Technology* **2005**, *37*, 19. (d) Gordon, C. M. *Appl. Catal*. **2001**, *222*, 101.
2. Fujita, K.; MacFarlane, D. R.; Forsyth, M. *Chem. Comm*. **2005**, 4804.
3. (a) Diego, T. De; Lozano, P.; Gmouth, S.; Vaultire, M.; Iborra, J. L. *Biomacromolecules* **2005**, *6*, 1457. (b) Rantwijk, F. van; Secundo, F.; Sheldon, R. A. *Green Chemistry* **2006**, *8*, 282.
4. Baker, S. N.; McCleskey, T. M.; Pandey, S.; Baker, G. A. *Chem. Comm*. **2004**, 940.
5. Biswas, A.; Shogren, R. L.; Stevenson, D. G.; Willett, J. L.; Bhowmik, P. K. *Carbohydrate Polymers* **2006**, *66*, 546.
6. Summers, C. A.; Flowers II, R. A. *Protein Science* **2000**, *9*, 2001.
7. Lange, C.; Patil, G.; Rudolph, R. *Protein Science* **2005**, *14*, 2693.
8. Haberler, M.; Schröder, C.; Steinhauser, O. *Phys. Chem. Chem. Phys*. **2011**, *13*, 6955.
9. Haberler, M.; Steinhauser, O. *Phys. Chem. Chem. Phys*. **2011**, *13*, 17994.
10. Tome, L. I. N.; Jorge, M.; Gomes, J. R. B.; Coutinho, J. A. P. *J. Phys. Chem. B* **2012**, *116*, 1831.
11. Cardoso, L.; Micaelo, N. M. *ChemPhysChem*. **2011**, *12*, 275.
12. Tateishi-Karimata, H.; Sugimoto, N. *Angew. Chem. Int. Ed.* **2012**, *51*, 1416.
13. Vijayaraghavan, R.; Izgorodin, A.; Ganesh, V.; Surianarayanan, M.; MacFarlane, D. R. *Angew. Chem. Int. Ed.* **2010**, *122*, 1675.
14. Klähn, M.; Lim, G. S.; Wu, P. *Phys. Chem. Chem. Phys*. **2011**, *13*, 18647.
15. Lozano, P.; Diego, T. de; Guegan, J. P.; Vaultier, M.; Iborra, J. L. *Biotechnol. Bioeng.* **2001**, *75*, 563.
16. Ulbert, O.; Bela-Bako, K.; Tonova, K.; Gubicza, L. *Biocatal. Biotransform*. **2005**, *23*, 177.
17. Persson, M.; Bornscheuer, U. T. *J. Mol. Catal. B: Enzym*. **2003**, *22*, 21.
18. Rios, A. P. de los; Hernandez-Fernandez, F. J.; Rubio, M.; Gomez, D.; Villora, G. *J. Chem. Technol. Biotechnol*. **2007**, *82*, 190.
19. Micaelo, N. M.; Soares, C. M. *J. Phys. Chem. B* **2008**, *112*, 2566.
20. Klähn, M.; Lim, G. S.; Wu, P. *Phys. Chem. Chem. Phys*. **2011**, *13*, 1649.
21. Llinás, M. *Metal-polypeptide Interactions: The Conformational State of Iron Proteins, Structure and Bonding* **1973**, *17*, 135.
22. Canongia Lopes, J. N.; Deschamps, J.; Padua, A. A. H. *J. Phys. Chem. B* **2004**, *108*, 2038; **2004**, *108*, 11250.
23. Dang, L. X.; Chang, T. M. *J. Chem. Phys*. **2002**, *106*, 235.
24. Kaminski, G.; Jorgensen, W. L. *J. Chem. Soc. Perkin Trans 2* **1999**, 2365.
25. Forster, T. R.; Smith, W. The DLPROTEIN 2.1 Reference Manual (Warrington, CCLRC, Daresbury Laboratory, 2001).
26. van Gunsteren, W. F.; Berendsen, H. J. C. Groningen Molecular Simulation (GROMOS) Library Manual, Biomos, (Groningen, 1987).
27. Forster, T. R.; Smith, W. The DLPOLY 2.13 Reference Manual (Warrington, CCLRC, Daresbury Laboratory, 2001).
28. Humphrey, W.; Dalke, A.; Schulten, K. VMD: Visual Molecular Dynamics *J. Mol. Graphics* **1996**, *14*, 33.
29. Endres, F.; MacFarlane, D.; Abbott, A. *Electrodeposition from Ionic Liquids*; Wiley: New York, 2008.
30. Shim, Y.; Jeong, D.; Manjari, S.; Choi, M. Y.; Kim, H. J. *Acc. Chem. Res*. **2007**, *40*, 1130.
31. Berendsen, H. J. C.; Grigera, J. R.; Straatsma, T. P. *J. Phys. Chem*. **1987**, *91*, 6269.
32. Luzar, A.; Soper, A. K.; Chandler, D. *J. Chem. Phys*. **1993**, *99*, 6836.
33. Benjamin, I. *J. Chem. Phys*. **1999**, *110*, 8070.
34. Kabsch, W. *Acta. Crystal.* **1976**, *32A*, 922; **1978**, *32A*, 827.
35. Danmjanović, A.; García-Moreno, B.; Lattman, E. E.; García, A. E. *PROTEINS; Structure, Function, and Bioinformatics* **2005**, *60*, 433.